

Highly Parallel Imaging: Hardware & Methods

Lawrence L. Wald, Ph.D.

Introduction: Advances in field strength and improved gradient performance have been substantial and are the image most practitioners have of advancing MR technology. Nonetheless, advances in the third component of the triad, RF technology, have proved as valuable and perhaps more cost-effective for improved sensitivity and encoding capabilities in MR imaging. The coils which come standard on a state of the art scanner today look very different from those of 15 years ago. For example, the single channel volume coil was a standard receive coil for brain, extremity and even body imaging. Today, array coils of 8 to 32 channels perform the receive function and birdcage structures are found only as transmit coils (and even the single channel transmit coil appears to have a limited future thanks to parallel transmit array technology.)

The complexity (and associated cost) of highly parallel detection is easy to see with a glance inside the covers of a 32 or higher channel coil array (e.g. Fig. 1, a 64 channel head/neck/C-spine array). So what is the benefit? The answers are sensitivity and encoding ability and the ability to trade-off these two desirable goals in a flexible way. This talk will largely focus on what can currently be done in this arena and what some of the technological barriers are faced. It will include a hardware overview of highly parallel arrays, issues such as how to measure SNR in arrays, and finally some recent parallel imaging methods that take advantage of 3D distribution of coils, such as Simultaneous MultiSlice (SMS) or MultiBand imaging.



Fig. 1 The loop layout of a close-fitting 64 channel head/neck/C-spine/vascular array for 3T. Left) with covers. Right) top and bottom section without covers. Far Right) SNR map. The SNR was improved in the brain cortex by 2.4x compared to a larger 20ch array and by 1.2x compared to a similar sized 32channel array. In the C-spine region the SNR was increased 1.8x compared to the 20ch head/neck array. Courtesy Boris Keil, MGH.

Combining the data from array coils

In his original paper, Roemer described a way to elegantly combine the data from the multiple receivers of the array.[1] It is almost always advantageous to combine the data from the multiple channels in the spatial domain since the sensitivity profiles of each individual array element can be a steep function of the pixel's coordinates. Then the optimization can be done on a pixel-by-pixel basis taking into account the spatially changing amplitudes and relative phases of the sensitivity profiles. In addition to measuring the coil signal map $S_i(x,y,z)$ for each element, i , which tells us how the signal vectors will add, we need to know the noise covariance matrix, Ψ , which describes the thermal noise variance in each channel and the covariance between pairs of channels, which informs us of how the noise from the channels adds. For a

given pixel, we can form a vector of the coil sensitivity, \mathbf{C} , and measured signal level, \mathbf{S} , for each channel. Here \mathbf{C} and \mathbf{S} exist for each pixel and are vectors of length N_{ch} . We then generate the image intensity, I , of the combined channels for that pixel from a normalized weighted sum of the measured signal levels. The weights will be chosen to maximize the SNR of the combined pixel. We also express the complex weights as a vector, \mathbf{w} , of length N_{ch} . Then the general expression is

$$I = \lambda \mathbf{w}^H \mathbf{S} \quad (1)$$

where λ is a normalization constant which might vary as a function of location but does not effect the pixels SNR. Roemer showed that if the noise variances are equal and uncorrelated (Ψ proportional to the identity matrix), then $\mathbf{w} = \mathbf{C}$ and

$$I = \lambda \mathbf{C}^H \mathbf{S}. \quad (2)$$

To create an image with spatially uniform noise levels, λ is chosen as

$$\lambda = \frac{1}{\sqrt{\mathbf{C}^H \mathbf{C}}} \quad (3)$$

When the noise correlation matrix is not simply the identity matrix (either the channel's variances are unequal, or shared noise or coupling exists in the array), then the combination is fully optimized; $\mathbf{w} = \Psi^{-1} \mathbf{C}$ then;

$$I^{optSNR} = \lambda \mathbf{C}^H \Psi^{-1} \mathbf{S} \quad (4)$$

and λ becomes as

$$\lambda = \frac{1}{\sqrt{\mathbf{C}^H \Psi \mathbf{C}}}. \quad (5)$$

This can be thought of as "pre-whitening" the signal vector \mathbf{S} prior to the combination (replacing \mathbf{S} with $\Psi^{-1} \mathbf{S}$). Roemer also showed that if the SNR is high in each channel, then the coil sensitivity vector \mathbf{C} is well approximated by the signal vector \mathbf{S} and does not need to be measured. I.e. the coil sensitivity is essentially just a map of the signal with perfect SNR. If the noise covariance is also proportional to the identity matrix and we use the λ for uniform noise, then we get what Roemer called the "root sum-of-squares" method;

$$I^{SoS} = \sqrt{\mathbf{S}^H \mathbf{S}}. \quad (6)$$

This is a particularly useful form because no pre-scan measurements are required of \mathbf{C} or Ψ . One simply takes the sum of the square of the signal levels of each channel's measurement of that pixel. Since the noise covariance matrix requires only a second to acquire (by digitizing noise in the absence of excitation), it is useful to add this information in, but preserve the estimation of \mathbf{C} by \mathbf{S} . Then we have the "covariance weighted root-sum-of-squares" combination: $I^{cov-SoS} = \lambda \mathbf{S}^H \Psi^{-1} \mathbf{S}$ with $\lambda = \sqrt{\mathbf{S}^H \Psi^{-1} \mathbf{S}}$, which simplifies to

$$I^{cov-SoS} = \sqrt{\mathbf{S}^H \Psi^{-1} \mathbf{S}}. \quad (7)$$

Given the choice of weights, w_i , the image SNR is given by[1]:

$$SNR = \frac{\mathbf{w}^H \mathbf{S}}{\sqrt{\mathbf{w}^H \Psi \mathbf{w}}}. \quad (8)$$

For the other combination methods, the resulting SNR can be shown to be:

$$SNR^{SoS} = \frac{\mathbf{S}^H \mathbf{S}}{\sqrt{\mathbf{S}^H \Psi \mathbf{S}}}, \quad (9)$$

while the image SNR for the noise cov-SoS is

$$\text{SNR}^{\text{cov rSoS}} = \sqrt{S^T \Psi^{-1} S} . \quad (10)$$

Note that the SNR for the covariance weighted sum-of-squares image is (remarkably) the same as the image itself.

Assessing SNR in arrays In the combination methods above, the complex-valued weights are chosen to maximize the image SNR using the coil sensitivity profiles and noise covariance matrix (or estimates thereof). The problem with the simple noise ROI in the “black” background area of an image is that usually there is no estimate of the coil sensitivities in this region. This results in sub-optimum combination of the array elements in this region and an amplification of the noise by an unknown factor. For example, if the rSoS method is used, the channels are essentially weighted by noise and combined. This is of little concern for discrimination of anatomy, since the weights used inside the body are accurate, but it eliminates this easy method of ROI outside the head to measure noise. Note the ROI in the noise-only part of the image is perfectly valid for single channel coils (after correction for the Rician distribution in magnitude data[2] or if the coil sensitivity is known in that region (for example through a theoretical calculation) and used to combine the data there.

Assessing the SNR of an image acquired with an array coil in a manner that can be readily compared to either another group’s measurements or to the SNR obtained by analyzing the signal mean and variance of a time-series of images requires further considerations. Kellman and McVeigh[3] elegantly described the series of correction factors needed to produce SNR in “absolute units”, which are exactly what is needed to make the calculated SNR maps agree with those obtained from a time-series measurement and subsequently to make SNR maps directly comparable. When these correction factors are used, the SNR measurement some important book-keeping is performed and scale factors accounted for so the SNR maps can be compared from site to site. Four factors are outlined and described in detail. The first defines a “noise equivalent bandwidth” of the receiver, which differs slightly from manufacturer to manufacturer and provides a factor that accounts for the “real” bandwidth of the measurement. The second factor accounts for noise averaging by the Fourier Transform by normalizing the noise covariance matrix by the number of samples contributing to the image. The third factor is a simple $\sqrt{2}$ which arises since the observation model assumes the noise is real valued while the noise is complex valued. The final correction factor, needs to be applied to account for the incorrect assumption of Gaussian noise statistics in magnitude images. [4] This correction factor applies to the SNR map formed from the rSoS combination, since the individual channels are converted to magnitude maps prior to combination. Then the correction factor is a function of the number of channels and the SNR value thus it must be applied pixel by pixel. It is a generalization of the well-known Rician distribution correction [2] to multichannel rSoS combined arrays, which follow a non-central chi distribution, with $2n$ degrees of freedom, where n is the number of coils, and is a potentially larger correction[4]. Although often considered unimportant for images with SNR above 10, this correction factor can be significant for highly parallel arrays even for typical SNR levels. For example, the noise statistic bias correction lowers the measured SNR by a factor of 0.6 for a 32-channel acquisition in an image with SNR = 13.

Finally, the use of parallel image reconstructions (accelerated imaging) further complicates analysis of image SNR. It introduces spatially-variant noise amplification in the reconstructed images, leading to image SNR degradation associated with the acceleration factor and the coil’s geometry factor (g-factor). The latter has become an attractive figure of merit for assessing the performance of coil arrays for parallel image encoding. While simple methods exist for

calculating the noise enhancement in SENSE reconstruction[5, 6], for GRAPPA, the equivalent of the g-factor calculation has only been recently addressed [7, 8].

Anatomy of an array coil.

The loop coil forms a magnetic dipole reception pattern, which couples primarily to magnetic fields in the near-field region. Namely, the alternating external flux produced by the spins induces an EMF in the loop through Faraday's law. An isolated coil element has resistive losses from its conducting wires, solder joints, losses in the dielectric material of the capacitors and eddy-current losses in any surrounding structures. For a coil near a conductive sample the losses arising from induced eddy currents (from dB/dt) and displacement currents in the sample volume typically dominate all other losses. The fraction of losses dissipated in the body relative to the components is easily measured by comparing the unload Quality factor (Q) of the coil to the loaded Q . Since $Q = \omega L/R$ for an LCR circuit, it is easy to show that $R_{body}/R_{comp} = Q_{UL}/Q_L - 1$. Since body noise is detected through the same mechanism and at the same frequency as the MR signal (Faraday detection at the Larmor frequency), the two cannot be distinguished and efforts to improve the signal detection will necessarily increase the noise level. In this respect, maximum body noise means maximum MR signal with the added benefit that other loss (and therefore noise) sources become negligible. For example, if a $Q_{UL}/Q_L = 6$ is achieved, then component losses are 5 fold smaller than the body losses and eliminating them completely will improve the image SNR by less than 10%. If $Q_{UL}/Q_L = 10$, elimination of the component losses (e.g. through super conductors etc) improves SNR by a factor of 1.005. This gives the coil engineer a clear picture of when s/he can stop worrying about component losses. The eddy currents and capacitive coupling to the body also produce shifts in resonance frequency upon loading. The principle method for controlling the resonance shifts is to distribute the capacitors around the loop, using multiple large capacitors rather than a single small one.

During RF excitation, provided by a uniform body transmit coil, the receiver coil must be detuned to reduce the power transmitted into the Rx chain during Tx. In addition to potentially damaging sensitive electronic components, large currents induced in the Rx coil could also create SAR hotspots of their own and cause heating and injury. Thus, the receiver coil must be "transparent", i.e., it must not distort the B_1^+ profile of the volume excitation coil during Tx. This can be achieved by limiting the induced currents to negligible levels by switching on high impedance elements in the coil loop. In the most common configuration an detuning trap circuit under active control is incorporated into the loop. This comprises a PIN diode and a series inductor which resonates at the Larmor frequency across one of the capacitors from the loop. The diode acts as a switch connecting the parallel resonant trap to the coil, thus, inserting a high impedance parallel

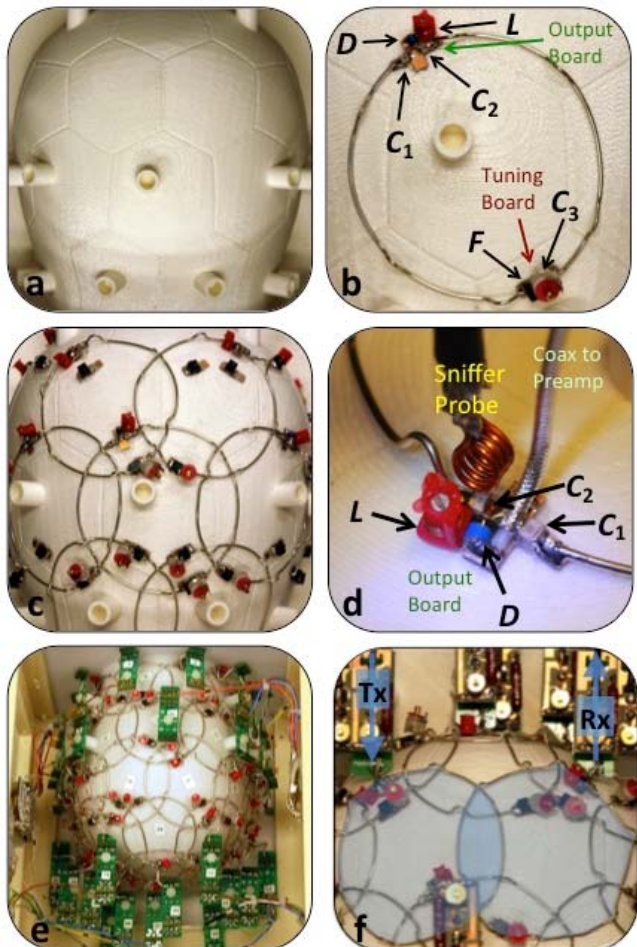


Fig. 1 Detailed look at the construction of a highly parallel array.

LC circuit in series in the loop. As a redundant safety feature, passive elements are often also employed incase the active system fails. One popular passive device is to bridge a second LC trap with passive crossed diodes or to use an RF fuse in the loop.

While MR coil engineers typically prefer to work with arrays with little or no mutual coupling, there is some evidence that modest decoupling is relatively unimportant if the image is combined with either the cov-rSoS or optimal-SNR method.[9] These methods already utilize the noise covariance matrix, as do accelerated image reconstruction methods like SENSE. The greatest fear of the beginning coil builder is that the coupling will perturb the resonance frequency of the carefully tuned high-Q resonators rendering them insensitive to the Larmor frequency. We show below that this fear is ungrounded when preamplifier decoupling is used. Nevertheless, coupling between multiple elements makes it difficult to transform the impedance of the element to that which optimizes the preamplifier noise figure. In addition, noise in the preamplifier can project back into the coil and then couple to other elements. This added noise appears on the diagonals of the noise covariance matrix and is therefore not mitigated with inclusion of the matrix. [10] Finally we note that at some point, if all the elements are coupled enough to give identical profiles, parallel MRI reconstructions will become highly ill-conditioned; i.e. the sensitivity patterns contain less distinct spatial information than the uncoupled coils would.

References

1. Roemer, P.B., W.A. Edelstein, C.E. Hayes, S.P. Souza, and O.M. Mueller, *The NMR phased array*. Magn Reson Med, 1990. 16(2): p. 192-225.
2. Gudbjartsson, H. and S. Patz, *The Rician distribution of noisy MRI data*. Magnetic resonance in medicine : official journal of the Society of Magnetic Resonance in Medicine / Society of Magnetic Resonance in Medicine, 1995. 34(6): p. 910-4.
3. Kellman, P. and E.R. McVeigh, *Image reconstruction in SNR units: a general method for SNR measurement*. Magnetic resonance in medicine : official journal of the Society of Magnetic Resonance in Medicine / Society of Magnetic Resonance in Medicine, 2005. 54(6): p. 1439-47.
4. Constantinides, C.D., E. Atalar, and E.R. McVeigh, *Signal-to-noise measurements in magnitude images from NMR phased arrays*. Magn Reson Med, 1997. 38(5): p. 852-7.
5. Pruessmann, K.P., M. Weiger, and P. Boesiger, *Sensitivity encoded cardiac MRI*. J Cardiovasc Magn Reson, 2001. 3(1): p. 1-9.
6. Pruessmann, K.P., M. Weiger, M.B. Scheidegger, and P. Boesiger, *SENSE: sensitivity encoding for fast MRI*. Magn Reson Med, 1999. 42(5): p. 952-62.
7. Blaimer, M., F.A. Breuer, N. Seiberlich, M.F. Mueller, R.M. Heidemann, V. Jellus, G. Wiggins, L.L. Wald, M.A. Griswold, and P.M. Jakob, *Accelerated volumetric MRI with a SENSE/GRAPPA combination*. J Magn Reson Imaging, 2006. 24(2): p. 444-50.
8. Robson, P.M., A.K. Grant, A.J. Madhuranthakam, R. Lattanzi, D.K. Sodickson, and C.A. McKenzie, *Comprehensive quantification of signal-to-noise ratio and g-factor for image-based and k-space-based parallel imaging reconstructions*. Magnetic resonance in medicine : official journal of the Society of Magnetic Resonance in Medicine / Society of Magnetic Resonance in Medicine, 2008. 60(4): p. 895-907.

9. Duensing, G.R., H.R. Brooker, and J.R. Fitzsimmons, *Maximizing signal-to-noise ratio in the presence of coil coupling*. Journal of magnetic resonance. Series B, 1996. 111(3): p. 230-5.
10. Findelee, R., G.R. Duensing, and A. Reykowski. *Simulating array SNR & effective noise figure in dependence of noise coupling*. in *Proc. of the ISMRM*. 2011. Montreal Canada. 1883